European Spine Journal (2021) 30:1509–1520
https://doi.org/10.1007/s00586-021-06796-2

ORIGINAL ARTICLE

Sonic Hedgehog modulates the inflammatory response and improves functional recovery after spinal cord injury in a thoracic contusion–compression model

Hao Zhang[1] · Alexander Younsi[1] · Guoli Zheng[1] · Mohamed Tail[1] · Anna-Kathrin Harms[1] · Judith Roth[1] · Maryam Hatami[2] · Thomas Skutella[2] · Andreas Unterberg[1] · Klaus Zweckberger[1]

Received: 7 July 2020 / Revised: 15 January 2021 / Accepted: 24 February 2021 / Published online: 11 March 2021

Abstract

Purpose The Sonic Hedgehog (Shh) pathway has been associated with a protective role after injury to the central nervous system (CNS). We, therefore, investigated the effects of intrathecal Shh-administration in the subacute phase after thoracic spinal cord injury (SCI) on secondary injury processes in rats.

Methods Twenty-one Wistar rats were subjected to thoracic clip-contusion/compression SCI at T9. Animals were randomized into three treatment groups (Shh, Vehicle, Sham). Seven days after SCI, osmotic pumps were implanted for seven-day continuous intrathecal administration of Shh. Basso, Beattie and Bresnahan (BBB) score, Gridwalk test and bodyweight were weekly assessed. Animals were sacrificed six weeks after SCI and immunohistological analyses were conducted. The results were compared between groups and statistical analysis was performed ($p < 0.05$ was considered significant).

Results The intrathecal administration of Shh led to significantly increased polarization of macrophages toward the anti-inflammatory M2-phenotype, significantly decreased T-lymphocytic invasion and significantly reduced resident microglia six weeks after the injury. Reactive astrogliosis was also significantly reduced while changes in size of the posttraumatic cyst as well as the overall macrophagic infiltration, although reduced, remained insignificant. Finally, with the administration of Shh, gain of bodyweight (216.6 ± 3.65 g vs. 230.4 ± 5.477 g; $p = 0.0111$) and BBB score (8.2 ± 0.2 vs. 5.9 ± 0.7 points; $p = 0.0365$) were significantly improved compared to untreated animals six weeks after SCI as well.

Conclusion Intrathecal Shh-administration showed neuroprotective effects with attenuated neuroinflammation, reduced astrogliosis and improved functional recovery six weeks after severe contusion/compression SCI.

Keywords Spinal cord injury · Sonic Hedgehog · Neuroprotection · Inflammation · Functional recovery

Abbreviations

ANOVA	Analysis of variance
BBB	Basso, Beattie and Bresnahan
CNS	Central nervous system
PBS	Phosphate-buffered saline
ROI	Region of interest
SCI	Spinal cord injury
SEM	Standard error of the mean
Shh	Sonic Hedgehog

Introduction

Despite decades of research, spinal cord injury (SCI) remains a disastrous event, often associated with patients' lifelong disability and high socioeconomic costs [1, 2]. After the primary injury, a cascade of secondary injury processes is initiated in the spinal cord, leading to further degeneration of neural and glial cells, exacerbation of myelin damage, formation of cystic cavities and thus expansion and aggravation of the traumatic lesion [3, 4]. The resulting hostile microenvironment is thereby exceedingly linked to a distinct ongoing neuroinflammatory response with, e.g., macrophagic

Hao Zhang and Alexander Younsi contributed equally to this work.

✉ Alexander Younsi
alexander.younsi@med.uni-heidelberg.de

[1] Department of Neurosurgery, University Hospital Heidelberg, INF 400, 69120 Heidelberg, Germany

[2] Department of Neuroanatomy, Institute for Anatomy and Cell Biology, University of Heidelberg, INF 307, 69120 Heidelberg, Germany

infiltration and polarization, invasion of T-lymphocytes, microglial activation and reactive astrogliosis until chronic postinjury stages [5, 6]. Experimental treatment strategies aiming to attenuate such secondary injury processes and thus to improve functional recovery after SCI have been the focus of many preclinical studies, but the results have been varying and translation into the clinical practice has been proven to be difficult [4, 7]. As an alternative approach to reduce the sequelae of SCI, the enhancement of existing but limited endogenous mechanisms of neuroprotection and repair has evolved into an intriguing concept [8, 9]. Hereby, the secreted glycoprotein, Sonic hedgehog (Shh), which has been intensively studied in the context of embryonic notochord development has gained particular attention [10, 11]: Shh is a multifunctional growth factor that exerts its various functions through its binding with the smoothened and patched transmembrane proteins [12, 13]. During embryogenesis of neural tissue, it promotes, among other things, the differentiation of progenitor cells toward the neuronal or oligodendrocyte lineage while inhibiting the astrocyte lineage [14, 15]. Recently, ongoing mitogenic activity of Shh during adulthood in response to neural tissue injuries such as ischemia or trauma has been postulated [16, 17]. Moreover, the administration of exogenous Shh has led to increased survival and proliferation of endogenous neural and oligodendrocyte precursors in animal models of SCI, potentially also improving functional recovery [18–20]. The effects of Shh on the secondary injury processes after SCI remain, however, largely unknown. In our current study, we, therefore, aimed to assess the neuroprotective capacity of intrathecally administered Shh for the attenuation of the neuroinflammatory response, astrogliosis and cyst formation after thoracic contusion/compression SCI in rats with possible implications for functional recovery.

Materials and methods

Animals, experimental groups and study design

A total of 21 female Wistar rats (160 g; *Janvier Labs, France*) were randomly assigned to three treatment groups: Group 1 (Shh; $n=8$), group 2 (Vehicle; $n=8$) and group 3 (Sham; $n=5$). Assignment for groups 1 and 2 took place directly after SCI. For housing, 1815 cm^2 cages were used with a 12-h light–dark cycle, a temperature of 26 °C, food and water ad libitum and no possibility for self-training. Weighing of the animals was performed daily. Neurological function was assessed at baseline and weekly after SCI by three independent observers until the end of the experiment. Osmotic micropumps for the i.t. administration of Shh/Vehicle were implanted seven days after SCI. The experiment was terminated with the perfusion of all animals six weeks after SCI. All surgeries and outcome assessments were blinded, and all experimental protocols were approved by the Animal Care Committee of the federal government.

Surgical procedures

Animals were anesthetized with isoflurane (1.5–3%) and a 1:1 mixture of O_2 and N_2O for all surgical procedures.

A contusion–compression model with a 28-g modified aneurysm clip (*Fehlings Laboratory, Canada*) was used to induce a thoracic SCI at the T9 level, similar to the cervical SCI previously described by our group [6, 21]. In short, a laminectomy of T9 was performed, the clip was applied around the spinal cord, snap shut, and sustained for 60 s in all Shh and Vehicle animals (groups 1 and 2). Animals in the Sham group (group 3) only received a laminectomy of T9.

Administration of Shh/Vehicle into the intrathecal space was initiated seven days after SCI. To this end, a skip-laminectomy of T11 was performed and a rat intrathecal microcatheter (*Alzet, USA*), connected to a subcutaneous osmotic micropump (model 1007D; *Alzet, USA*), was subdurally placed with its open tip upon the epicenter of the lesion. The pumps had been filled with either 100 µl of Shh (50 ng/ml; *R&D Systems, USA* [22]*;*) or Vehicle (0.9% NaCl) and had been subjected to a 2-h preloading cycle at room temperature. After implantation, they continuously delivered Shh/Vehicle into the intrathecal space for seven days in all injured animals (group 1 and 2). Sham animals (group 3) only received a skip-laminectomy of T11.

After both surgical procedures, analgesics (0.05 mg/kg buprenorphine s.c.; *Bayer, Germany* and 2 mg/kg meloxicam s.c.; *Boehringer-Ingelheim, Germany*) as well as fluids (3–5 ml 0.9% NaCl s.c.) were administered for 3–5 days and animals received extensive care, nutritional support and antibiotic prophylaxis (4 mg/kg moxifloxacin p.o.; *Alcon, USA*) for 7 days. If necessary, bladders were manually expressed twice a day until the bladder reflexive function had recovered.

Assessment of weight and neurological function

Animals were weighed with a digital platform scale and daily bodyweight (in g) was recorded. The results were averaged for the baseline (one value per animal) and for every week after SCI (seven daily values per animal).

The Basso–Beattie–Bresnahan locomotor rating scale (BBB) was used to evaluate the general hindlimb locomotion recovery weekly over the course of the experiment. Hereby, hindlimb movement, joint movement, stepping, coordination, trunk and tail position as well as weight support of rats placed into an open field were evaluated for 4 min using a rating scale with scores from 0 to 21 points [23].

The Gridwalk test was additionally performed to assess fine sensory motor coordination. To this end, animals were placed on a 1-m-long pathway of randomly placed metal grids. The number of stepping errors defined as misplacement of a hind limb not on but between the bars was counted and averaged over four runs [24].

Animal perfusion and tissue processing

At the end of the experiment, six weeks after SCI, animals were deeply anesthetized with isoflurane (5%) and transcardially perfused with 50 ml 0.1 M cold phosphate-buffered saline (PBS) followed by 150 ml paraformaldehyde (4% in 0.1 M PBS at pH 7.4). Spinal cords were removed, post-fixed in 4% paraformaldehyde for 24 h and cryoprotected in 30% sucrose for 48 h. Pieces with a length of 1 cm, centered around the lesion epicenter, were then dissected from the spinal cord and placed into tissue embedding medium (*Sakura Finetek Europa B.V., Netherlands*) on dry ice. Consecutive spinal cord cross sections (every 240 µm) with a thickness of 30 µm were cut with a cryostat (*Leica Biosystems, Germany*), dried and stored at − 80 °C until further processing.

Immunofluorescence staining

Spinal cord sections were blocked with a blocking solution containing 5% non-fat milk powder, 1% bovine serum albumin and 0.3% Triton-X100 in 0.1 M PBS (all *Sigma-Aldrich, USA*) for 1 h at room temperature. The following primary antibodies, diluted in the same blocking solution, were then added and incubated at 4 °C overnight: Anti-Iba1 (1:200; *Novus Biologicals, USA*) for macrophages, anti-iNOS (1:100; *Abcam, USA*) for M1-macrophages, anti-CD206(1:200; *Bio-Rad, Germany*) for M2-macrophages, anti-TMEM119 (1:200; *Abcam, USA*) for microglia, anti-CD3 (1:200; *Bio-Rad, Germany*) for T-Lymphocytes and anti-GFAP (1:250; *Abcam, USA*) for astrocytes. Isotype controls with non-specific immunoglobulin at the same concentration were performed to ensure the specificity of the antibodies (data not shown).

As secondary antibodies, Alexa Fluor 405 donkey anti-goat (1:400; *Abcam, USA*), Alexa Fluor 557 donkey anti-mouse (1:400; *R&D Systems, USA*) and Alexa Fluor 647 donkey anti-rabbit (1:400; *Abcam, USA*), diluted in blocking solution without Triton-X100, were used and applied for 1 h at room temperature before covering the sections with mounting medium.

Imaging analysis

All immunofluorescence staining images were captured using a confocal laser microscope (LSM 700; *Carl-Zeiss, Germany*) with the ZEN microscope software (ZEN 2010*; Carl Zeiss, Germany*) at 10 × magnification in the 8-bit-format. Three wavelength channels (Alexa Fluor 405 nm, Alexa Fluor 557 nm, Alexa Fluor 647 nm) were used.

Quantitative assessment of macrophagic infiltration ($Iba1^+$ cells), macrophagic polarization into the M1- ($Iba1^+$/$iNOS^+$ cells) and the M2-phenotype ($CD206^+$/$iNOS^-$ cells), T-lymphocytic invasion ($CD3^+$ cells) and microglial activation ($TMEM119^+$ cells) was performed in six randomly selected Shh and Vehicle animals (groups 1 and 2) as well as all Sham animals (group 3). To this end, a semiautomatic cell-counting algorithm for ImageJ2 (National Institute of Health; *Bethesda, USA*) was used on seven spinal cord cross-sectional images per animal which had distinct distances to the lesion epicenter (0 µm, ± 240 µm, ± 480 µm and ± 720 µm): Briefly, the images were split into single channels, a Gaussian-blur filter (Sigma: 10.00) was applied to reduce background noise, and a selected region of interest (ROI) was transformed into a binary image with the "IsoData-thresholding" function. ROIs consisted of the entire spinal cord without the cyst and the autofluorescence border and their area (in μm^2) was additionally noted. Labeled cells were then counted in the selected ROI with the "Analyze Particles" function (with specific thresholds for each antibody). In case of co-labeling, binary images were recombined using the "Image Calculator" function, and the co-stained cells within the same ROI were counted. To reduce the inclusion of artifacts, only structures with an area of 50–2000 μm^2 were considered. The number of positively stained or co-stained cells per ROI/cross section was presented as the cell density (cells/mm^3) and the results were averaged per animal and per group.

For quantitative assessment of astrogliosis, the immunointensity of GFAP was measured on seven distinct spinal cord cross-sectional images (0 µm, ± 240 µm, ± 480 µm and ± 720 µm from the lesion epicenter) in six randomly selected Shh and Vehicle animals as well as all Sham animals. In short, images were split into single channels with the ImageJ2 software, ROIs were drawn around the entire spinal cord with exclusion of the cyst as well as the autofluorescence border, and the "Measure" function was used to output the integrated density (immunointensity) of the GFAP staining. The results were averaged per animal and per group.

The volume of a posttraumatic cyst was assessed on the same seven GFAP-stained spinal cord cross sections in the same six animals. To this end, ROIs were drawn around the posttraumatic cystic cavity, the area was calculated by applying the "Measure" function, multiplied by the section thickness (30 µm) and then averaged per animal and treatment group. The results are given in mm^3.

All quantitative imaging analyses were performed by two independent investigators blinded to treatment groups. For

qualitative assessment of tissue or cell morphology, additional images were obtained at 40 × magnification.

Statistical analysis

All the results are presented as mean ± standard error of the mean (SEM) per treatment group if not stated otherwise. Shapiro–Wilk normality tests were performed prior to all parametric analyses. For the statistical comparison of animal weight as well as BBB scores and Gridwalk test results between groups and time points, repeated measure two-way analyses of variance (ANOVAs) with Geisser–Greenhouse correction followed by Tukey's multiple comparison test with individual variances computed for each comparison were used. Means between multiple groups in the quantitative imaging analyses were compared using either Welch ANOVAs followed by Dunnett's T3 multiple comparison tests with individual variances computed for each comparison (normality test passed) or Kruskal–Wallis tests followed by Dunn's multiple comparison tests (normality test failed). For the comparison of means between two groups, an unpaired t-test with Welch's correction was used. All statistical analyses were performed using the software Prism (Version 7.0; *GraphPad Software, USA*) and p-values of $p < 0.05$ were considered significant.

Results

Macrophagic infiltration and polarization

To evaluate the inflammatory response after SCI, we quantified the infiltration of macrophages on spinal cord cross sections stained for the macrophagic marker Iba1 (Fig. 1a + b). The thoracic contusion–compression SCI led to a significant increase of $Iba1^+$ macrophages in the spinal cord of Shh animals (group 1; 10,532 ± 2163 cells/mm^3; Fig. 1c) and Vehicle animals (group 2; 8019 ± 1478 cells/mm^3; Fig. 1c) compared to Sham animals (group 3; 617 ± 135 cells/mm^3; $p = 0.0111$ and $p = 0.0158$, respectively; Fig. 1a) six weeks after the injury. Although animals in the Vehicle group showed the highest density of infiltrated macrophages, the difference to Shh-treated animals remained insignificant ($p = 0.7171$). Thus, we concluded that while increased macrophagic infiltration is present in the injured spinal cord six weeks after thoracic contusion/compression SCI, the i.t. administration of Shh is unable to modulate this aspect of neuroinflammation.

As the polarization of macrophages into different phenotypes plays an important role during the inflammatory response, we additionally quantified the density of pro-inflammatory M1-macrophages ($Iba1^+/iNOS^+$ cells; Fig. 2a–d) and anti-inflammatory M2-macrophages ($CD206^+/iNOS^-$ cells; Fig. 2f–j) in the perilesional spinal cord tissue. While the density of M1-macrophages was the highest in Vehicle animals (6169 ± 1197 cells/mm^3; Fig. 2e), treatment with Shh led to less M1-macrophages

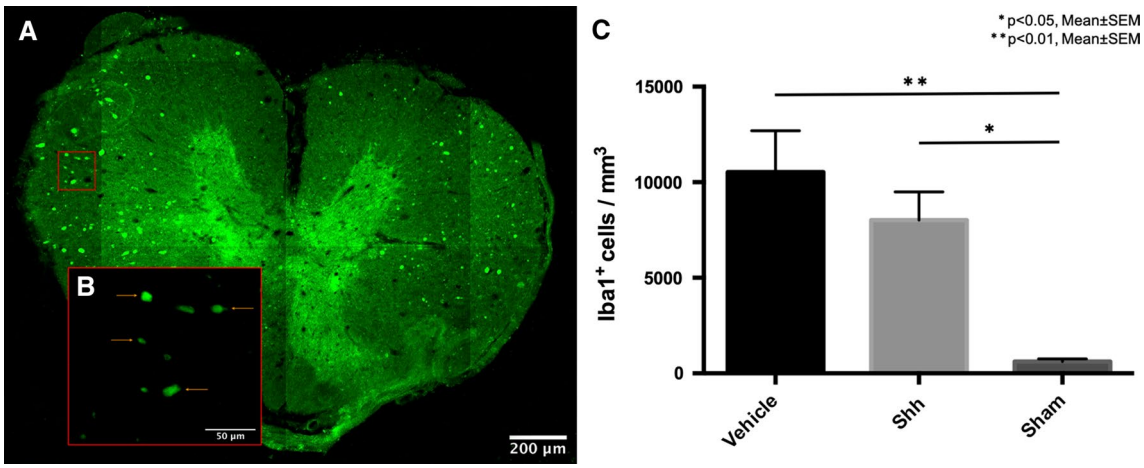

Fig. 1 Infiltration of macrophages into the spinal cord six weeks after thoracic SCI. **a** Spinal cord cross section stained for Iba1 (green), a marker for macrophages (10 × magnification). **b** Enlargement of the red framed inset in (**a**); orange arrows depicting the cell morphology (40 × magnification). **c** Animals in the Vehicle group as well as in the Shh group showed significantly more $Iba1^+$ macrophages compared Sham animals ($n = 5$–6/group; Welch ANOVA with Dunnett's T3 multiple comparison test; $p = 0.0111$ and $p = 0.0158$, respectively). Although less infiltration of macrophages was observed in the Shh group compared to the Vehicle group, this difference remained insignificant

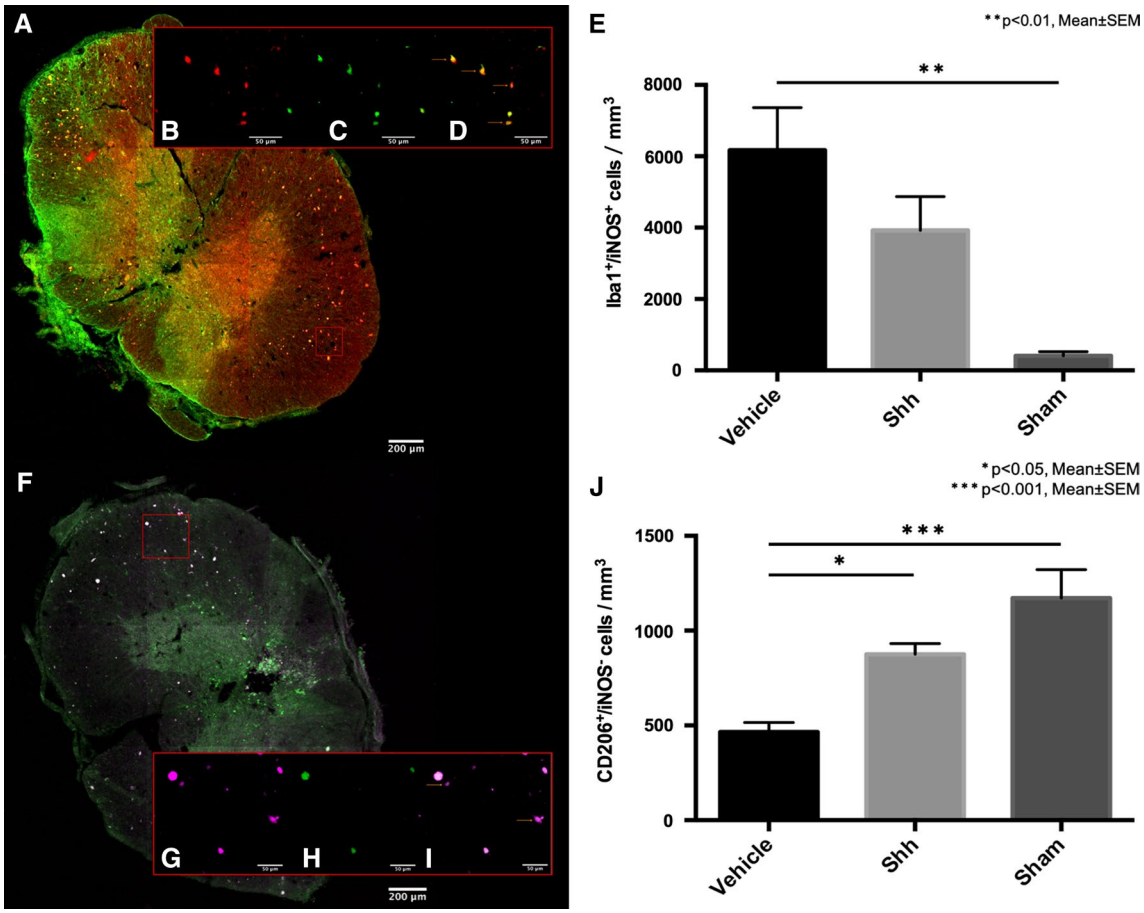

Fig. 2 Polarization of macrophages into the pro-inflammatory M1- and the anti-inflammatory M2-phenotype in the spinal cord six weeks after thoracic SCI. **a** Spinal cord cross section stained for Iba1 (red) and iNOS (green; 10×magnification). **b–d** Enlargement of the red framed inset in (**a**); colocalization of $Iba1^+$ macrophages (red) with the marker enzyme iNOS (green), indicating M1 polarized pro-inflammatory macrophages ($Iba1^+/iNOS^+$ cells; orange arrows; 40×magnification). **e** Animals in the Vehicle group showed significantly more pro-inflammatory M1-macrophages compared to the Sham group ($p=0.0131$), whereas the difference between Shh and Sham animals remained insignificant ($n=5$–6/group; Welch ANOVA with Dunnett's T3 multiple comparison test). **f** Spinal cord cross section stained for the macrophage mannose receptor CD206 (magenta) and iNOS (green; 10×magnification). **g–i** Enlargement of the red framed inset in (**f**); missing colocalization of $CD206^+$ macrophages (magenta) with iNOS (green), indicating M2 polarized anti-inflammatory macrophages ($CD206^+/iNOS^-$ cells; orange arrows; 40×magnification). **j** Animals in the Shh group showed significantly less anti-inflammatory M2-macrophages compared to the Vehicle group ($p=0.0008$), while no significant difference to the Sham group could be observed. Vehicle animals on the other hand had significantly less M2-macrophages compared to uninjured Sham animals ($p=0.0176$; $n=5$–6/group, Welch ANOVA with Dunnett's T3 multiple comparison test)

in the Shh group (3925 ± 945; Fig. 2e) without reaching a statistically significant difference ($p=0.4140$). However, Vehicle animals showed significantly more M1-macrophages compared to the uninjured Sham animals (441 ± 114 cells/mm^3; $p=0.0131$; Fig. 2e) whereas the difference between Shh animals and Sham animals remained insignificant ($p=0.0569$). Vice versa, the density of anti-inflammatory M2-macrophages was the lowest in the Vehicle group, while treatment with Shh resulted in significantly more M2-macrophages in the Shh group (466 ± 49 vs. 876 ± 56 cells/mm^3; $p=0.0008$; Fig. 2f). With 1172 ± 1501 $CD206^+/iNOS^-$ cells/mm^3 (Fig. 2f), the uninjured Sham animals showed a significantly higher density of M2-macrophages compared to the Vehicle animals ($p=0.0176$), but not compared to the Shh animals ($p=0.2943$). These results demonstrated that the i.t. administration of Shh is able to reduce the polarization of macrophages toward the pro-inflammatory M1-phenotype, but at the same time significantly increases their polarization toward the anti-inflammatory M2-phenotype six weeks after SCI.

Invasion of T-lymphocytes

The presence of T-lymphocytes in the injured spinal cord as a further aspect of neuroinflammation was assessed by quantification of $CD3^+$ cells (Fig. 3a + b). The density of

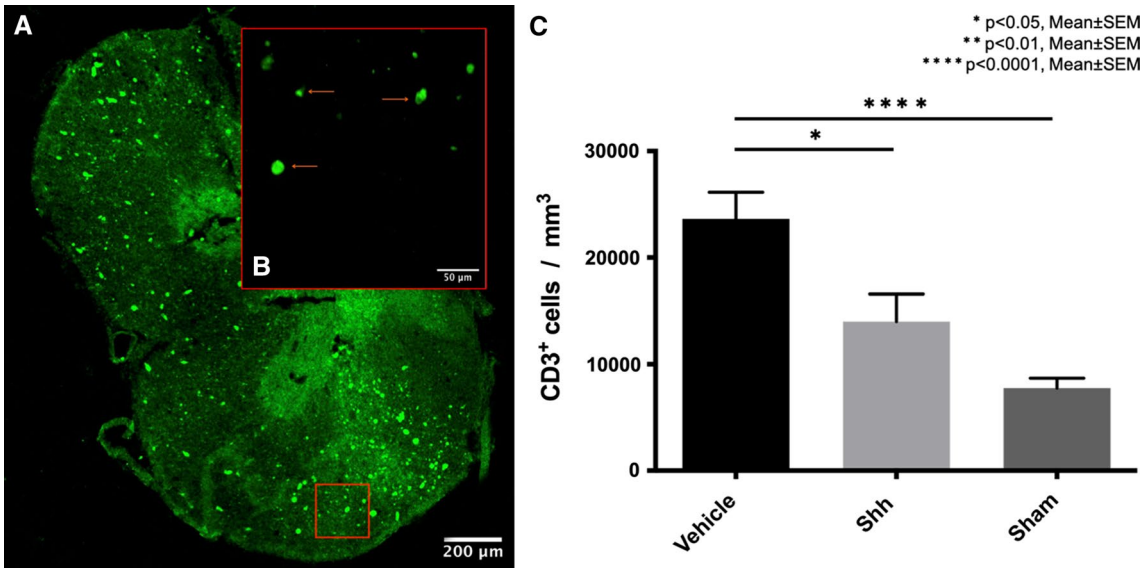

Fig. 3 Invasion of T-lymphocytes into the spinal cord six weeks after thoracic SCI. **a** Spinal cord cross section stained for CD3 (green), a marker for T-lymphocytes (10 × magnification). **b** Enlargement of the red framed inset in (**a**); orange arrows depicting the cell morphology (40 × magnification). **c** Animals in the Shh group showed significantly less $CD3^+$ T-lymphocytes compared to Vehicle animals ($p = 0.0433$) but no significant difference between Shh and uninjured Sham animals could be observed. Invasion of T-lymphocytes in the Vehicle group was, however, significantly increased compared to the Sham group ($p = 0.0026$; $n = 5$–6/group, Welch ANOVA with Dunnett's T3 multiple comparison test)

$CD3^+$ T-lymphocytes was found to be significantly lower in uninjured Sham animals (group 3; 7762 ± 916 cells/mm^3; Fig. 3c) compared to Vehicle animals (group 2; $23{,}648 \pm 2480$ cells/mm^3; $p = 0.0026$; Fig. 3a), but not compared to Shh animals (group 1; $14{,}000 \pm 2597$ cells/mm^3; $p = 0.1623$; Fig. 3c). Moreover, animals in the Shh group showed significantly less T-lymphocytes then animals in the Vehicle group ($p = 0.0433$). We assumed that the i.t. administration of Shh significantly reduces T-lymphocytic invasion of the injured tissue as part of the inflammatory response six weeks after SCI.

Microglial activation

Activation of the microglia in the injured spinal cord was measured on cross sections stained for the microglia marker TMEM119 (Fig. 4a + b). Quantification of the density of $TMEM119^+$ microglia cells showed a significant reduction in Shh animals (group 1) compared to Vehicle animals (group 2; $34{,}232 \pm 6466$ vs. $54{,}551 \pm 2098$ cells/mm^3; $p = 0.0443$; Fig. 4c). Animals in the Sham group (group 3), however, had the lowest density of microglia cells ($17{,}718 \pm 1039$ cells/mm^3; Fig. 4c) with a significant difference to the Vehicle ($p < 0.0001$) but not to the Shh animals ($p = 0.1328$). For this reason, we concluded that the i.t. administration of Shh significantly attenuates the perilesional microglial activation six weeks after SCI.

Reactive astrogliosis and cyst formation

The proliferation of GFAP-labelled astrocytes which are involved in the regulation of neuroinflammation was measured as the immunointensity of GFAP on spinal cord cross sections (Fig. 5a). GFAP immunointensity was hereby the lowest in the uninjured Sham animals (group 3; 16 ± 1.5; Fig. 5b), but showed a significant increase in injured Vehicle animals (group 2; 64 ± 6; $p < 0.0001$; Fig. 5b) as well as injured Shh animals (group 1; 41 ± 2; $p < 0.0001$; Fig. 5b). More importantly, the immunointensity of GFAP was also significantly higher in Vehicle animals compared to Shh animals ($p = 0.0323$). These results demonstrated that the i.t. administration of Shh is able to significantly reduce the reactive gliosis in the injured spinal cord six weeks after SCI.

The formation of cystic cavities in the injured spinal cord which act as a physical barrier for axonal regeneration and sprouting was assessed on the same spinal cord cross sections stained for GFAP. Such cystic cavities were present in all injured Shh and Vehicle animals (Fig. 5a), but they were generally smaller in the Shh group (group 1) compared to the Vehicle group (group 2; 2.422 ± 0.3811 mm^3 vs. 2.92 ± 0.6347 mm^3) without reaching a statistically significant difference ($p = 0.5200$; Fig. 5c). Thus, the i.t. administration of Shh does not significantly affect the formation of posttraumatic cysts six weeks after SCI.

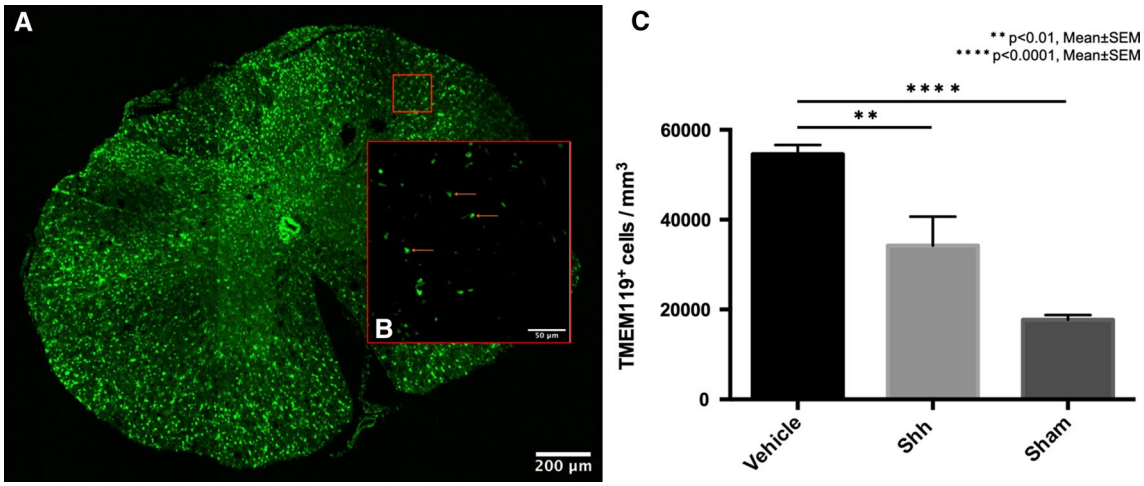

Fig. 4 Activation of resident microglia in the spinal cord six weeks after thoracic SCI. **a** Spinal cord cross section stained for TMEM119 (green), a marker for resident microglia (10×magnification). **b** Enlargement of the red framed inset in (**a**); orange arrows depicting the cell morphology (40×magnification). **c** Animals in the Shh group showed significantly less TMEM119$^+$ cells compared to Vehicle animals ($p=0.0443$). Activation of resident microglia was, however, the lowest in Sham animals with a significant difference to the Vehicle but not to the Shh animals ($n=5$–6/group; Welch ANOVA with Dunnett's T3 multiple comparison test; $p<0.0001$)

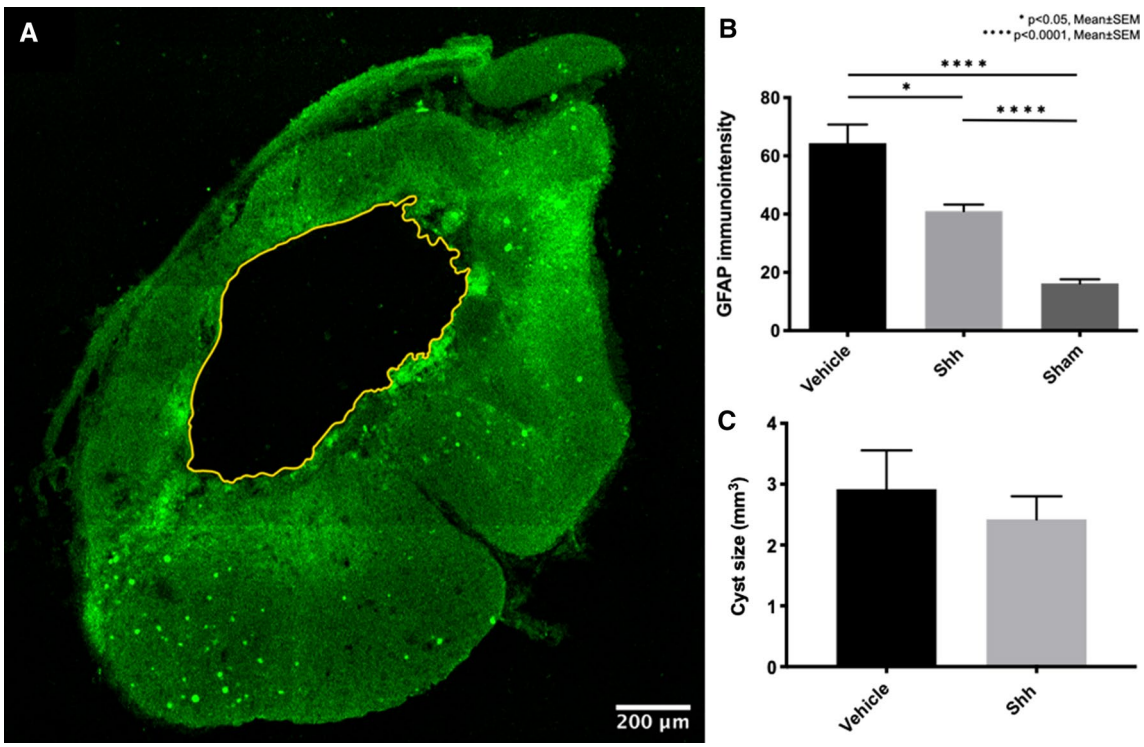

Fig. 5 Reactive astrogliosis and size of the posttraumatic cyst in the spinal cord six weeks after thoracic SCI. **a** Spinal cord cross section stained for GFAP (green), a marker for astrocytes, with a ROI (yellow) drawn around the intramedullary, posttraumatic cyst (10×magnification). **b** The immunointensity of the GFAP-staining was lowest in uninjured Sham animals and a significant increase in the reactive astrogliosis in Vehicle animals but also Shh animals could be observed ($n=5$–6/group; Kruskal–Wallis tests with Dunn's multiple comparison test; both $p<0.0001$). With the administration of Shh in the Shh group, reactive gliosis was significantly reduced compared to the untreated Vehicle group ($p=0.0323$). **c** Although cystic cavities in the injured spinal cord were smaller in Shh animals compared to Vehicle animals, this difference remained insignificant ($n=5$–6/group; unpaired t-test with Welch's correction)

Functional recovery

As a surrogate marker for functional recovery, we compared the weight gain of the animals in the different treatment groups over the course of the experiment. A continuous weight gain could be observed in all animals which resulted in a significant increase in the mean overall weight from 160.9 ± 0.1917 g at baseline to 232.8 ± 4.449 g in week six after SCI ($p < 0.0001$). While the toll of the injury was illustrated by a significantly lower weight of Vehicle and Shh animals (groups 2 and 1) compared to Sham animals (group 3) starting from week one until the end of the experiment, a significant difference in bodyweight could also be observed between animals in the Vehicle and the Shh group, favoring the Shh-treated animals from week four after SCI onwards (week 4: 195 ± 3.306 g vs. 208.7 ± 1.973 g, $p = 0.0111$; week 5: 208.9 ± 3.805 g vs. 220.6 ± 2.819 g, $p = 0.0341$; week 6: 216.6 ± 3.65 g vs. 230.4 ± 5.477 g, $p = 0.0111$; Fig. 6a). Hence, we concluded that the i.t. administration of Shh leads to a significant gain of bodyweight in the later stages after SCI, indicating better recovery.

To assess general locomotor recovery of the hindlimbs, the 21-point BBB open field score was performed at baseline prior to and weekly after SCI. While the maximum of 21 points was reached by all animals in the BBB at baseline, the contusion/compression SCI at the T9 level had a devastating effect on the hindlimb locomotion in Shh (group 1) and Vehicle (group 2) animals during the first week after injury, represented by mean BBB scores of 0.1429 ± 0.1429 and 0.125 ± 0.125 points, respectively (Fig. 6b). Despite this high injury severity, BBB scores continuously improved in all injured animals over the course of the experiment and reached a maximum of 8.214 ± 0.1844 points in the Shh group and 5.938 ± 0.7161 in the Vehicle group six weeks after SCI without plateauing, yet (Fig. 6b). Animals in the Sham group (group 3) consistently achieved 21 points in the BBB at every time point and the difference in hindlimb locomotor function to Shh as well as Vehicle animals therefore remained significant until the end of the experiment (data not shown). Animals in the Shh group achieved significantly higher BBB scores compared to animals in the Vehicle group from week three after SCI onwards (week 3: 2.714 ± 0.3058 vs. 1.5 ± 0.2835 points; $p = 0.0310$; week 4: 4.357 ± 0.4325 vs. 3.25 ± 0.4725 points; $p = 0.0231$; week 5: 6.571 ± 0.2974 vs. 4.938 ± 0.6369 points; $p = 0.0498$; and week 6: 8.214 ± 0.1844 vs. 5.938 ± 0.7161 points; $p = 0.0365$; Fig. 6b). These results suggested that the i.t. administration of Shh significantly improves locomotor recovery of the hindlimbs in later stages after SCI showing only its maximal effect by the end of the experiment. Despite these positive effects of the Shh-treatment, functional recovery during the first six weeks after the thoracic clip contusion/compression injury was still very limited, and animals were rarely able to bear their own weight (BBB score > 8).

Fine sensory and motor movements, as well as general coordination, were further evaluated with the Gridwalk test which was performed at baseline prior to and weekly after SCI. While animals in the Sham group (group 3) exhibited neither stepping errors at baseline, nor at any other time point, the thoracic contusion/compression injury was so severe that the Gridwalk test could not be performed during the first week after SCI due to the inability of the injured

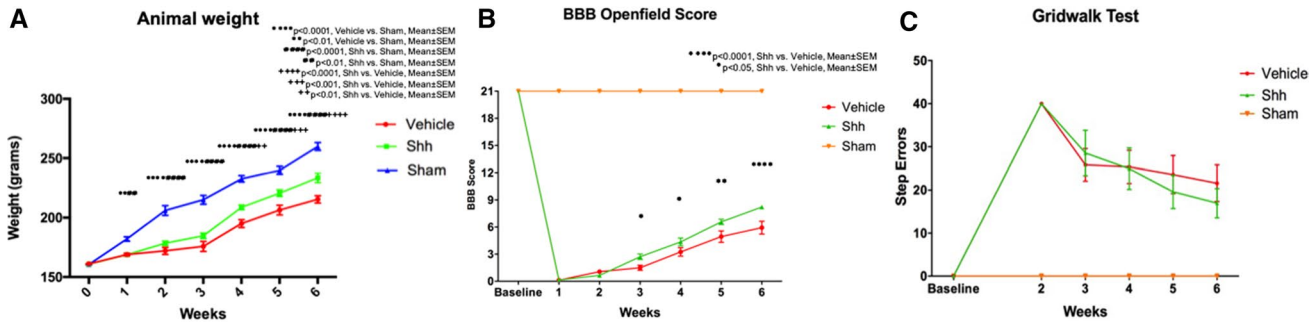

Fig. 6 Changes of bodyweight, general locomotor recovery and coordination from baseline until six weeks after thoracic SCI. **a** Animals in the Sham group showed a significantly higher bodyweight compared to Vehicle but also Shh animals starting from week one after SCI until the end of the experiment. A significant difference in bodyweight could also be observed between the lighter Vehicle animals and the heavier Shh animals in weeks four ($p = 0.0111$), five ($p = 0.0341$) and six ($p = 0.0111$) after SCI ($n = 5$–8/group; repeated measure two-way ANOVA with Geisser–Greenhouse correction followed by Tukey's multiple comparison test). **b** While hindlimb locomotion was drastically impaired in both, Vehicle and Shh animals, during the first two weeks after SCI, the Shh group performed significantly better as the Vehicle group from week three after SCI onwards ($p = 0.0310$, $p = 0.0231$, $p = 0.0498$ and $p = 0.0365$; $n = 5$–8/group; repeated measure two-way ANOVA with Geisser–Greenhouse correction followed by Tukey's multiple comparison test). **c** Assessment of fine sensory and motor movements as well as coordination with the Gridwalk test revealed no significant differences between the Vehicle and the Shh animals over the course of the experiment although the number of stepping errors as lower in the Shh group compared to the Vehicle group at week five and six after SCI ($n = 5$–8/group; repeated measure two-way ANOVA with Geisser–Greenhouse correction followed by Tukey's multiple comparison test)

animals to move. At week two after SCI, animals in the Shh group (group 1), as well as the Vehicle group (group 2), were able to cross the Gridwalk, but they showed errors with every single step (both 40 ± 0 stepping errors/run; Fig. 6c). Thereafter, stepping errors tended to decrease in the injured animals, and in week three after SCI, the Vehicle group showed slightly fewer stepping errors compared to the Shh group (25.83 ± 3.758 stepping errors/run vs. 28.58 ± 5.276 stepping errors/run; Fig. 6c). While Vehicle and Shh animals performed similarly at week four after SCI (25.38 ± 3.834 stepping errors/run vs. 24.96 ± 4.806 stepping errors/run), stepping errors were less frequent in Shh animals compared to Vehicle animals at week five after SCI (24.96 ± 4.806 stepping errors/run vs. 23.58 ± 4.404 stepping errors/run), as well as at the end of the experiment (16.96 ± 3.409 stepping errors/run vs. 21.58 ± 4.245 stepping errors/run; Fig. 6c). Despite the clear trend toward improved fine sensory and motor movements in Shh-treated animals at weeks five and six after SCI, no statistically significant differences could be achieved. This led us to the assumption that an observation period of up to six weeks after SCI might be too short to detect beneficial effects of the i.t. treatment with Shh on improved sensory motor coordination.

Discussion

While the widely conserved Hedgehog pathway is primarily involved in morphogenesis, neuronal guidance and angiogenesis during embryonal development, it has also been associated with vascular proliferation and regeneration in adult tissues [25–27]. In the CNS, morphogenic events are predominantly linked to Sonic Hedgehog (Shh) signaling, whereby secreted Shh binds and inactivates the transmembrane receptor Patched-1 (Ptch-1) which then releases its inhibitory effect on Smoothend (Smo) allowing the induction of target genes through the Gli family of transcription factors [28, 29]. After injury to the adult CNS, an overexpression of Shh has been observed and it has been postulated that Shh might play an essential role for gliogenesis and neurogenesis, two important aspects of tissue repair [22, 30]. In the context of SCI, Shh has mainly been studied as an exogenous factor to enhance proliferation and differentiation of endogenous progenitor cells which are still present in the adult spinal cord [31]. Bambakidis et al. were able to show in several in vivo experiments that the administration of Shh directly into the spinal cord or intravenously led to increased proliferation of endogenous neuronal and oligodendrocyte precursors after moderate contusion SCI in rats [18, 20, 22, 32]. Similarly, Lowry et al. observed increased proliferation of endogenous oligodendrocyte lineage cells after contusion as well as hemi-section SCI and long-term administration of Shh via implanted biodegradable microspheres in mice [19]. Thomas et al. on the other hand used multiple channel bridges for lentiviral Shh-gene delivery to the injured tissue after hemi-section SCI in mice and reported axon extension and remyelination by endogenous progenitor cells [33]. While a proliferative effect of exogenous Shh-administration on the endogenous progenitor cells in the spinal cord after SCI, therefore, seems established, no data is currently available on its impact on secondary injury processes in the injured tissue such as the inflammatory response, astrogliosis and the formation of a posttraumatic cyst.

In our current study, we have used a severe contusion/compression model to induce a thoracic SCI in rats which was associated with severe impairment of the neurologic function and is considered closely simulating the clinical reality of human SCI [21, 34, 35]. Seven days after the injury, we have then initiated continuous administration of exogenous Shh into the subdural space over the lesion epicenter via an osmotic micropump for another seven days. The starting point of the Shh-administration in the subacute phase after SCI was thereby chosen due to several considerations: Firstly, we expected a higher potential of the neuroregenerative effects of the Shh signaling after the acute postinjury phase with its contusion, blood–spinal cord barrier disintegration and edema formation. Secondly, our strategy of intrathecal Shh-application required a second surgery which could not be performed early after SCI due to the reduced state of the animals and the increased risk of perioperative morbidity and complications. Thirdly, we had to optimize our intervention for possible translation into the clinical practice, requiring a stabilized situation and enough time to overcome logistical challenges [36]. The duration of the Shh-administration was subject to the protein's rapid clearance from the CNS as well its short-lived effects on a cellular level which require prolonged application with a constant concentration [19, 37]. Six weeks after SCI, we observed significantly improved functional recovery in Shh-treated animals. More importantly, we assessed effects of Shh on secondary injury processes and could show that the polarization of macrophages toward the anti-inflammatory M2-phenotye, the level of T-lymphocytic invasion of the injured tissue as well as the perilesional microglial response, all part of the inflammatory changes after SCI, were significantly improved. In addition, reactive astrogliosis in the injured spinal cord was significantly reduced with Shh-treatment.

The association between astrocytes and the Shh-pathway has been investigated by several researchers and it has been postulated that astrocytes have the ability to produce Shh as a response to CNS injury, which in turn reduces the gliogenic response and increases the proliferation of, e.g., oligodendrocytes [16, 19]. For that reason, we assume that the administration of exogenous Shh into the perilesional tissue might have increased this determination of glial cells away

from astrocytic proliferation, thus resulting in reduced reactive gliosis after Shh-treatment in our study [38]. Another effect of exogenous Shh might have been the overexpression of Netrin 1 by the CNS endothelium, a protein that is critical for stabilizing the blood–brain barrier (BBB) and limiting immune cell infiltration after CNS injury [39]. Already under homeostatic conditions, astrocyte-secreted Shh has been shown to induce Netrin 1 expression which in turn upregulates the presence of tight- and adherents junction molecules in the BBB, limiting immune cell infiltration [40]. An explanation for the reduced number of migrated T-lymphocytes and macrophages after Shh-administration in our study, therefore, could be the Shh-mediated stabilization of the blood–spinal cord barrier via Netrin 1. On the other hand, Shh has been identified as a macrophage chemoattractant during the immune response in other tissues such as the gut [41], somehow contradicting our results of reduced infiltration of macrophages in the spinal cord. However, we could additionally show an effect of Shh on the polarization of macrophages toward the anti-inflammatory M2-phenotype, and furthermore, treatment with Shh had also decreased the number of $TMEM119^{+}$ resident microglia cells in our experiment, suggesting further Shh-mediated inflammatory processes in the CNS that are not yet fully understood [42].

Despite the severity of the contusion/compression model used in our experiment, we were able to show a significant difference in functional recovery six weeks after SCI between Shh and Vehicle animals. To our knowledge, such a considerable impact of a treatment with Shh has rarely been observed in the context of SCI in the literature, although less severe injury models have often been used. The attenuated inflammatory response and the reduced astrogliosis we observed might have contributed to the success of the Shh-treatment in our study. However, additional effects of Shh in the injured spinal cord likely have played an even greater role for functional recovery: Shh has been linked to improved remyelination [16, 33], bFGF and VEGF expression [43], axonal sprouting [19] and synaptic plasticity [44]. All those pleiotropic actions, induced by a single protein, make Shh an excellent candidate for the treatment of a complex disease such as SCI, which likely requires combinatorial approaches [45]. Especially due to its simultaneous impact on secondary injury processes and cellular proliferation, Shh should be further assessed as a valuable adjunct to stem cell transplantation after SCI.

Conclusion

In our current study, the continuous, intrathecal administration of exogenous Shh for seven days after thoracic severe contusion/compression SCI led to long-lasting attenuation of the inflammatory response with significantly increased polarization of macrophages toward the anti-inflammatory M2-phenotype, significantly decreased T-lymphocytic invasion and significantly reduced resident microglia six weeks after the injury. With the Shh-treatment, reactive astrogliosis was also significantly reduced in this chronic stage of SCI while changes in size of the posttraumatic cyst as well as the overall macrophagic infiltration, although reduced, remained insignificant. With the administration of exogenous Shh, functional recovery, measured by gain of bodyweight as well as changes in the BBB score, was significantly improved in the later stages after SCI as well. While Shh has mostly been associated with proliferation of endogenous progenitor cells after SCI, we provide novel data on its effect as a neuroprotective agent on secondary injury processes. Given its pleiotropic properties, Shh seems to be a valid candidate for the treatment of a complex disease such as SCI and should be further assessed in future studies.

Acknowledgments The authors acknowledge the help of Dr. Claudia Pitzer and Barbara Kurpiers from the Interdisciplinary Neurobehavioral Core (INBC) Facility at the University of Heidelberg with animal housing, surgery, care and testing of neurological function as well as the help of Ilse C. Wagner with correcting the manuscript.

Authors contributions HZ performed the experiment, analyzed the results and co-wrote the manuscript. AY designed the study, performed the experiment, analyzed and interpreted the results and co-wrote the manuscript. GZ performed the experiment, analyzed the results and corrected the manuscript. MT performed the experiment and corrected the manuscript. JR performed the experiment and corrected the manuscript. AK performed the experiment and corrected the manuscript. MH corrected the manuscript. TS provided resources and material for the experiment and corrected the manuscript. AU provided resources and material for the experiment and corrected the manuscript. KZ designed the study, supervised the experiment and corrected the manuscript.

Funding Open Access funding enabled and organized by Projekt DEAL.

Declarations

Conflicts of interest The authors declares that they have no competing interest.

Data availability All data analyzed during the current study are available from the corresponding author on reasonable request.

References

1. Furlan JC, Sakakibara BM, Miller WC, Krassioukov AV (2013) Global incidence and prevalence of traumatic spinal cord injury. Can J Neurol Sci 40:456–464. https://doi.org/10.1017/S0317167100014530
2. Sekhon LH, Fehlings MG (2001) Epidemiology, demographics, and pathophysiology of acute spinal cord injury. Spine. https://doi.org/10.1097/00007632-200112151-00002
3. Mothe AJ, Tator CH (2013) Review of transplantation of neural stem/progenitor cells for spinal cord injury. Int J Dev Neurosci 31:701–713. https://doi.org/10.1016/j.ijdevneu.2013.07.004
4. Ahuja CS, Nori S, Tetreault L et al (2017) Traumatic spinal cord injury - repair and regeneration. Clin Neurosurg 80:S22–S90. https://doi.org/10.1093/neuros/nyw080
5. Hausmann ON (2003) Post-traumatic inflammation following spinal cord injury. Spinal Cord 41:369–378. https://doi.org/10.1038/sj.sc.3101483
6. Riemann L, Younsi A, Scherer M et al (2018) Transplantation of neural precursor cells attenuates chronic immune environment in cervical spinal cord injury. Front Neurol 9:1–12. https://doi.org/10.3389/fneur.2018.00428
7. Donnelly DJ, Popovich PG (2008) Inflammation and its role in neuroprotection, axonal regeneration and functional recovery after spinal cord injury. Exp Neurol 209:378–388. https://doi.org/10.1016/j.expneurol.2007.06.009
8. Bambakidis NC, Theodore N, Nakaji P et al (2005) Endogenous stem cell proliferation after central nervous system injury: alternative therapeutic options. Neurosurg Focus 19:E1. https://doi.org/10.3171/foc.2005.19.3.2
9. Yamamoto S, Yamamoto N, Kitamura T et al (2001) Proliferation of parenchymal neural progenitors in response to injury in the adult rat spinal cord. Exp Neurol 172:115–127. https://doi.org/10.1006/exnr.2001.7798
10. Ruiz I Altaba A, Palma V, Dahmane N (2002) Hedgehog-Gli signalling and the growth of the brain. Nat Rev Neurosci. 3:24–33. https://doi.org/10.1038/nrn704
11. Krauss S, Concordet JP, Ingham PW (1993) A functionally conserved homolog of the Drosophila segment polarity gene hh is expressed in tissues with polarizing activity in zebrafish embryos. Cell 75:1431–1444. https://doi.org/10.1016/0092-8674(93)90628-4
12. Kenney AM, Rowitch DH (2000) Sonic hedgehog promotes G1 cyclin expression and sustained cell cycle progression in mammalian neuronal precursors. Mol Cell Biol 20:9055–9067. https://doi.org/10.1128/mcb.20.23.9055-9067.2000
13. Miller RH, Hayes JE, Dyer KL, Sussman CR (1999) Mechanisms of oligodendrocyte commitment in the vertebrate CNS. Int J Dev Neurosci 17:753–763. https://doi.org/10.1016/S0736-5748(99)00068-4
14. Jessell TM (2000) Neuronal specification in the spinal cord: inductive signals and transcriptional codes. Nat Rev Genet 1:20–29
15. Sussman CR, Davies JE, Miller RH (2002) Extracellular and intracellular regulation of oligodendrocyte development: roles of sonic hedgehog and expression of E proteins. Glia 40:55–64. https://doi.org/10.1002/glia.10114
16. Amankulor NM, Hambardzumyan D, Pyonteck SM et al (2009) Sonic hedgehog pathway activation is induced by acute brain injury and regulated by injury-related inflammation. J Neurosci 29:10299–10308. https://doi.org/10.1523/JNEUROSCI.2500-09.2009
17. Androutsellis-Theotokis A, Leker RR, Soldner F et al (2006) Notch signalling regulates stem cell numbers in vitro and in vivo. Nature 442:823–826. https://doi.org/10.1038/nature04940
18. Bambakidis NC, Horn EM, Nakaji P et al (2009) Endogenous stem cell proliferation induced by intravenous hedgehog agonist administration after contusion in the adult rat spinal cord. J Neurosurg Spine 10:171–176. https://doi.org/10.3171/2008.10.SPI08231
19. Lowry N, Goderie SK, Lederman P et al (2012) The effect of long-term release of Shh from implanted biodegradable microspheres on recovery from spinal cord injury in mice. Biomaterials 33:2892–2901. https://doi.org/10.1016/j.biomaterials.2011.12.048
20. Bambakidis NC, Wang X, Lukas RJ et al (2010) Intravenous hedgehog agonist induces proliferation of neural and oligodendrocyte precursors in rodent spinal cord injury. Neurosurgery 67:1709–1715. https://doi.org/10.1227/NEU.0b013e3181f9b0a5
21. Younsi A, Zheng G, Scherer M et al (2020) Treadmill training improves survival and differentiation of transplanted neural precursor cells after cervical spinal cord injury. Stem Cell Res 45:101812. https://doi.org/10.1016/j.scr.2020.101812
22. Bambakidis NC, Wang R-Z, Franic L, Miller RH (2003) Sonic hedgehog-induced neural precursor proliferation after adult rodent spinal cord injury. J Neurosurg 99:70–75
23. Basso DM, Beattie MS, Bresnahan JC (1995) A sensitive and reliable locomotor rating scale for open field testing in rats. J Neurotrauma 12:1–21. https://doi.org/10.1089/neu.1995.12.1
24. Metz GAS, Merkler D, Dietz V et al (2000) Efficient testing of motor function in spinal cord injured rats. Brain Res 883:165–177. https://doi.org/10.1016/s0006-8993(00)02778-5
25. Fuccillo M, Joyner AL, Fishell G (2006) Morphogen to mitogen: the multiple roles of hedgehog signalling in vertebrate neural development. Nat Rev Neurosci 7:772–783. https://doi.org/10.1038/nrn1990
26. Nagase T, Nagase M, Machida M, Fujita T (2008) Hedgehog signalling in vascular development. Angiogenesis 11:71–77. https://doi.org/10.1007/s10456-008-9105-5
27. Byrd N, Grabel L (2004) Hedgehog signaling in murine vasculogenesis and angiogenesis. Trends Cardiovasc Med 14:308–313. https://doi.org/10.1016/j.tcm.2004.09.003
28. Chiang C, Litingtung Y, Lee E et al (1996) Cyclopia and defective axial patterning in mice lacking Sonic hedgehog gene function. Nature 383:407–413. https://doi.org/10.1038/383407a0
29. Østerlund T, Kogerman P (2006) Hedgehog signalling: how to get from Smo to Ci and Gli. Trends Cell Biol 16:176–180. https://doi.org/10.1016/j.tcb.2006.02.004
30. Wang Y, Imitola J, Rasmussen S et al (2008) Paradoxical dysregulation of the neural stem cell pathway sonic hedgehog-gli1 in autoimmune encephalomyelitis and multiple sclerosis. Ann Neurol 64:417–427. https://doi.org/10.1002/ana.21457
31. Horner PJ, Power AE, Kempermann G et al (2000) Proliferation and differentiation of progenitor cells throughout the intact adult rat spinal cord. J Neurosci 20:2218–2228. https://doi.org/10.1523/jneurosci.20-06-02218.2000
32. Bambakidis NC, Miller RH (2004) Transplantation of oligodendrocyte precursors and sonic hedgehog results in improved function and white matter sparing in the spinal cords of adult rats after contusion. Spine J 4:16–26. https://doi.org/10.1016/j.spinee.2003.07.004
33. Thomas AM, Seidlits SK, Goodman AG et al (2014) Sonic hedgehog and neurotrophin-3 increase oligodendrocyte numbers and myelination after spinal cord injury. Integr Biol (Camb) 6:694–705. https://doi.org/10.1039/c4ib00009a

34. Wilcox JT, Satkunendrarajah K, Zuccato JA et al (2014) Neural precursor cell transplantation enhances functional recovery and reduces astrogliosis in bilateral compressive/contusive cervical spinal cord injury. Stem Cells Transl Med 3:1148–1159. https://doi.org/10.5966/sctm.2014-0029
35. Zweckberger K, Ahuja CS, Liu Y et al (2016) Self-assembling peptides optimize the post-traumatic milieu and synergistically enhance the effects of neural stem cell therapy after cervical spinal cord injury. Acta Biomater 42:77–89. https://doi.org/10.1016/j.actbio.2016.06.016
36. Yamazaki K, Kawabori M, Seki T, Houkin K (2020) Clinical trials of stem cell treatment for spinal cord injury. Int J Mol Sci. https://doi.org/10.3390/ijms21113994
37. Bambakidis NC, Petrullis M, Xu K et al (2012) Improvement of neurological recovery and stimulation of neural progenitor cell proliferation by intrathecal administration of Sonic hedgehog. J Neurosurg 116:1114–1120. https://doi.org/10.3171/2012.1.JNS111285
38. Agius E, Soukkarieh C, Danesin C et al (2004) Converse control of oligodendrocyte and astrocyte lineage development by Sonic hedgehog in the chick spinal cord. Dev Biol 270:308–321. https://doi.org/10.1016/j.ydbio.2004.02.015
39. Alvarez JI, Dodelet-Devillers A, Kebir H et al (2011) The hedgehog pathway promotes blood-brain barrier integrity and CNS immune quiescence. Science 334:1727–1731. https://doi.org/10.1126/science.1206936
40. Alvarez JI, Darlington PJ, Prat A et al (2015) Netrin 1 regulates blood–brain barrier function and neuroinflammation. Brain 138:1598–1612. https://doi.org/10.1093/brain/awv092
41. Schumacher MA, Donnelly JM, Engevik AC et al (2012) Gastric sonic hedgehog acts as a macrophage chemoattractant during the immune response to Helicobacter pylori. Gastroenterology 142:1150–1159. https://doi.org/10.1053/j.gastro.2012.01.029
42. Bennett ML, Bennett FC, Liddelow SA et al (2016) New tools for studying microglia in the mouse and human CNS. Proc Natl Acad Sci U S A 113:E1738–E1746. https://doi.org/10.1073/pnas.1525528113
43. Jia Y, Wu D, Zhang R et al (2014) Bone marrow-derived mesenchymal stem cells expressing the Shh transgene promotes functional recovery after spinal cord injury in rats. Neurosci Lett 573:46–51. https://doi.org/10.1016/j.neulet.2014.05.010
44. Gulino R, Gulisano M (2012) Involvement of brain-derived neurotrophic factor and sonic hedgehog in the spinal cord plasticity after neurotoxic partial removal of lumbar motoneurons. Neurosci Res 73:238–247. https://doi.org/10.1016/j.neures.2012.04.010
45. Ratan RR, Noble M (2009) Novel multi-modal strategies to promote brain and spinal cord injury recovery. Stroke 40:130–132. https://doi.org/10.1161/STROKEAHA.108.534933